

Electronic Supplementary Information

Fast and sensitive fluorescent detection of inorganic mercury species and methylmercury using fluorescent probe based on displacement reaction of arylboronic acid with the mercury species

Lok Nath Neupane^a, Joohee Park^a, Pramod Kumar Mehta^a, Eun-Taex Oh^b, Heon Joo Park^b and Keun-Hyeung Lee^{a,*}

^aCenter for Design and Applications of Molecular Catalysts, Department of Chemistry and Chemical Engineering, Inha University, 100 Inha-Ro, Yonghyun-Dong, Nam-Gu, Incheon 402-751, South Korea

^bDepartment of Biomedical Sciences, College of Medicine, Inha University, Inha-Ro 100, Incheon city, 402-751, South Korea

E-mail: leekh@inha.ac.kr

Contents

1. Experimental Section	S3
1.1. Reagents	S3
1.2. synthesis of 1 and 2	S3
1.3. General fluorescence measurements	S4
1.4. Determination of detection limit	S4
1.5. HPLC-mass analysis of the products	S4
2. Figures	S5-S21
Scheme S1. Synthesis of compound 1	S5
Figure S1. HPLC Chromatogram of 1	S6
Figure S2. ESI-MS of 1	S7
Figure S3. HRMS (ESI-TOF) spectrum of 1	S8
Figure S4. ¹ H NMR of 1	S9
Figure S5. ¹³ C NMR of 1	S10
Figure S6. HPLC chromatogram of 2	S11
Figure S7. HRMS (ESI-TOF) spectrum of 2	S12
Figure S8. ¹ H NMR of 2	S13
Figure S9. ¹³ C NMR of 2	S14

Figure S10. Fluorescent spectrum and time-dependent emission intensity at 500 nm of 1 with Hg ²⁺	S15
Figure S11. Fluorescent spectrum and time-dependent emission intensity at 500 nm of 1 with various mercury salts	S16
Figure S12. Fluorescent spectra of 2 (10 μ M) with Hg ²⁺	S17
Figure S13. Linear intensity change of 1 as a function of HgCl ₂	S18
Figure S14. Fluorescent spectrum and time-dependent emission intensity at 500 nm of 1 with Hg ²⁺ and sequential addition of EDTA	S19
Figure S15. Mass analysis of the major peak in HPLC	S20
Figure S16. Partial ¹ H NMR spectra of 1 with HgCl ₂	S21
Figure S17. pH-dependent absorption/emission spectrum of 1	S22
Figure S18. UV-visible spectrum of 1 (10 μ M) with HgCl ₂	S23
Figure S19. (a) Fluorescent spectrum and (b) time-dependent emission intensity of 1 with CH ₃ HgCl	S24
Figure S20. HPLC analysis using C ₁₈ column for 1 with CH ₃ HgCl	S25
Figure S21. Mass analysis of the major peak in HPLC	S26
Figure S22. Cell image study of 1 with HgCl ₂ and CH ₃ HgCl	S27
Table S1. Comparison of the detection properties of fluorescent probes for methylmercury	S28
Table S2. Photo-physical data for 3 and 4 in various solvent	S29
References	S30

1. Experimental Section

1.1. Reagents:

Dansyl Chloride and, Aniline were purchased from TCI chemicals. 4 aminophenylboronic acid pinacol ester and Triethylamine were purchased from Sigma Aldrich.

1.2. Synthesis of 1 and 2

1.2.1 Synthesis of 1

Dansyl chloride (100 mg, 0.37 mmol) and triethylamine (155 μ L, 1.11 mmol) were added to a solution of 4-aminophenylboronic acid pinacol ester (77 mg, 0.35 mmol) in dichloromethane (10 mL). The reaction mixture was stirred at room temperature for 3 h, and the progress of the reaction was monitored by TLC. Upon completion of the reaction, Trifluoroacetic acid (268 μ L, 3.5 mmol) was added and the reaction mixture was stirred at room temperature for 2 h. The solvent was removed by rotary evaporator and the crude product was purified using silica gel column chromatography (eluent: EtOAc/hexane, 1:4, v/v) to give the product as a light yellow solid, **1**. Compound **1** with high purity was characterized by melting point, ESI-MS, ^1H NMR, and ^{13}C NMR spectroscopies.

Light yellow solid, yield 80%; M.P.: 162 $^{\circ}\text{C}$; ^1H NMR (DMSO- d_6) δ : 10.75 (s, 1H), 8.42 (d, J = 8.4 Hz, 1H), 8.36 (d, J = 8.8 Hz, 1H), 8.22 (d, J = 7.6 Hz, 1H), 7.62-7.57 (m, 2H), 7.52 (d, J = 9.2, 2H), 7.24 (d, J = 7.6, 1H), 6.97 (d, J = 8.4 Hz, 2H), 2.80 (s, 6H); ^{13}C NMR (DMSO- d_6) δ : 151.07, 139.39, 135.15, 134.8, 130.02, 128.98, 128.9, 128.3, 123.69, 118.94, 117.1, 115.56, 45.18; HRMS (m/z): $[\text{M} + \text{H}]^+$ calculated for $\text{C}_{18}\text{H}_{19}\text{BN}_2\text{O}_4\text{S}$: 371.1231, observed: 371.1231.

1.2.21 Synthesis of 2

Dansyl chloride (100 mg, 0.37 mmol) and triethylamine (155 μ L, 1.11 mmol) were added to a solution of 4-aminobenzene (37 μ L, 0.40 mmol) in dichloromethane (10 mL). The reaction mixture was stirred at room temperature for 3 h, and the progress of the reaction was monitored by TLC. The solvent was removed by rotary evaporator and the crude product was purified using silica gel column chromatography (eluent: EtOAc/hexane, 1:4, v/v) to give the product as a light yellow solid, **2**. Compound **2** with high purity was characterized by melting point, ESI-MS, ^1H NMR, and ^{13}C NMR spectroscopies.

Light yellow solid, yield 86%; M. P. , 121-122 $^{\circ}\text{C}$; ^1H NMR ($\text{CH}_3\text{CN}-d_3$) δ : 8.54-8.46 (m, J = 8.4 Hz, 2H), 8.27-8.23 (m, J = 8.8 Hz, 2H), 7.71 (t, J = 7.6 Hz, 1H), 7.60-7.56 (m, 1H), 7.52 (d, J = 8.4 Hz, 1H), 7.16-7.11 (m, 2H), 7.02-6.98 (m, 2H), 4.49 (brs, 1H), 2.97 (s, 6H); ^{13}C NMR ($\text{CH}_3\text{CN}-d_3$) δ : 147.44, 137.94, 135.95, 131.79, 130.18, 129.77, 129.13, 128.94, 125.70, 125.64, 123.14, 121.34, 46.49; HRMS (m/z): $[\text{M} + \text{H}]^+$ calculated for $\text{C}_{18}\text{H}_{18}\text{N}_2\text{O}_2\text{S}$: 327.1161, observed: 327.1160.

1.3 General fluorescence measurements

A stock solution of **1** (0.5×10^{-3} M) was prepared in CH₃CN and distilled water (1:1) and stored in a cold and dark place. The concentration of **1** was confirmed by UV absorbance at 330 nm for the dansyl group. A stock solution (500 μ M) of HgCl₂ was prepared in distilled water. A stock solution (1 mM) of CH₃HgCl was prepared in DMF. Fluorescence emission spectrum of a sample in a cuvette was measured in distilled water containing 1% CH₃CN or in aqueous buffered solution (10 mM HEPES, at pH 7.4) containing CH₃CN using a Perkin Elmer luminescence spectrophotometer (model LS 55). Emission spectra (400–700 nm) of the sample were measured by excitation with 380 nm.

1.4 Determination of detection limit

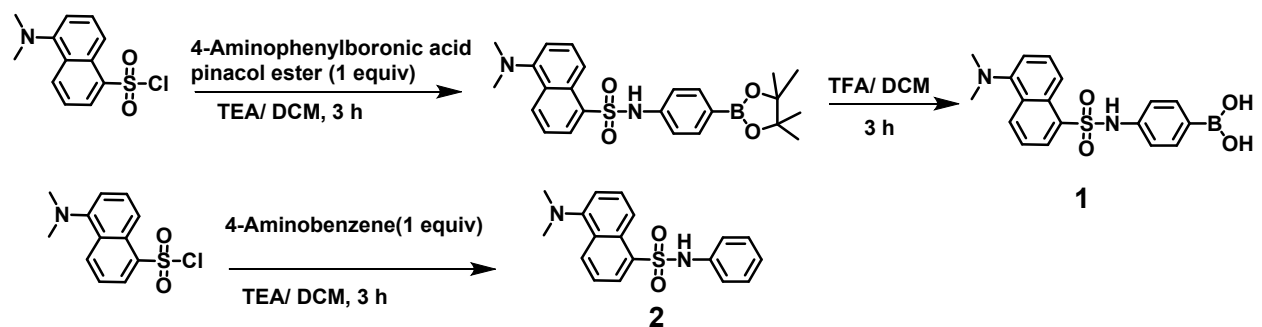
The detection limit was calculated based on the fluorescence titration. To determine the S/N ratio, the emission intensity of **1** without HgCl₂ was measured by ten times and the standard deviation of blank measurements was determined. Three independent duplication measurements of emission intensity were performed in the presence of HgCl₂ and each average value of the intensities was plotted as a concentration of HgCl₂ for determining the slope. The detection limit is then calculated with the following equation:

$$\text{Detection limit} = \frac{3\sigma}{m}$$

Where, σ is the standard deviation of blank measurements, m is the slope between intensity versus sample concentration.

1.5 HPLC-mass analysis of the reaction

The product of the reaction between **1** and HgCl₂ was analyzed by HPLC-MS (Thermo scientific Ultimate 3000 and MSQ plus) with a Agilent C18 column using a water (0.1% TFA)–acetonitrile (0.1% TFA) gradient. To a solution of **1** (10 μ M) in water (1 mL) containing 1% CH₃CN was added HgCl₂ (5 μ M) and incubates 20 min at room temperature. This reaction mixture was injected to the HPLC-MS and collected the data after run finished.



Scheme S1. Synthesis of **1** and **2**.

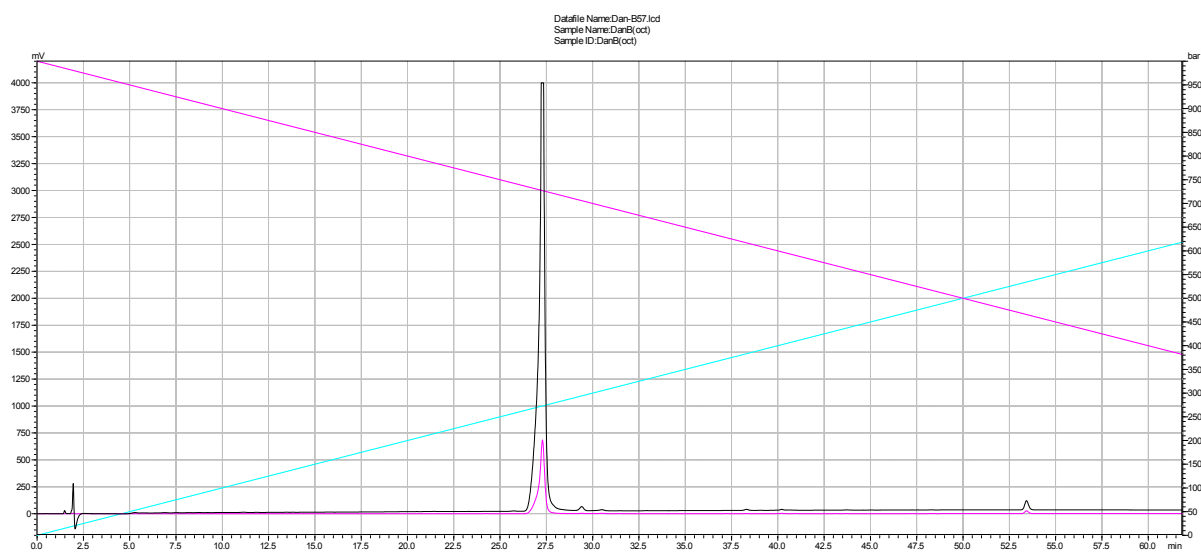


Figure S1. HPLC chromatogram of **1**. Black line and red line indicated the absorbance at 214 nm and 280 nm, respectively.

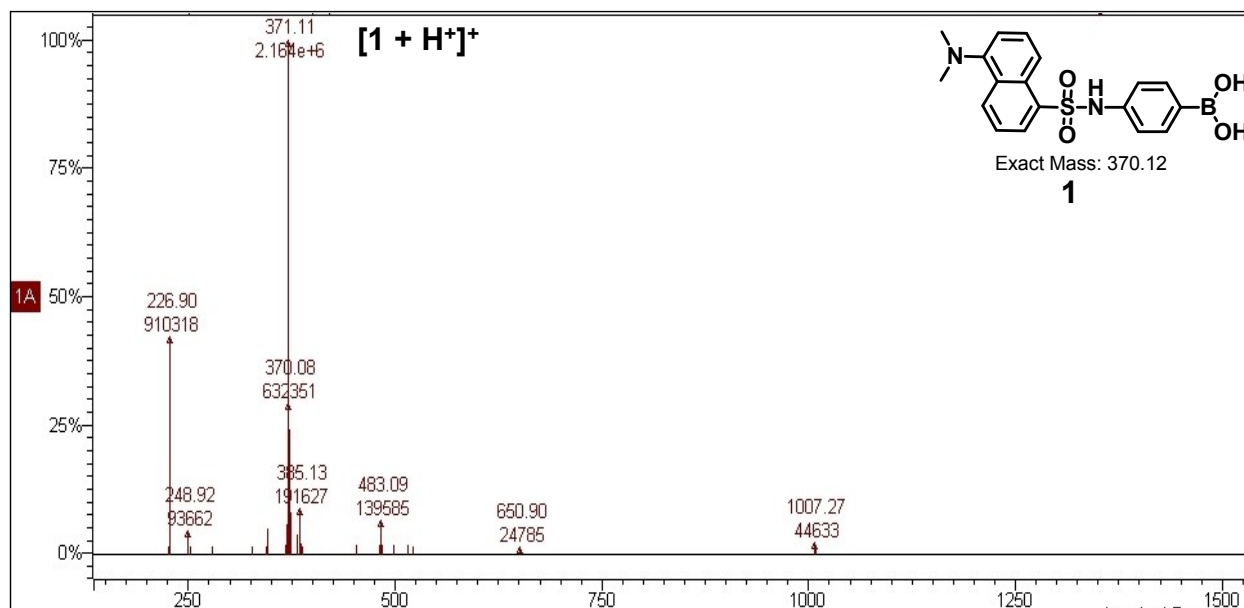


Figure S2. ESI-mass spectrum of **1**.

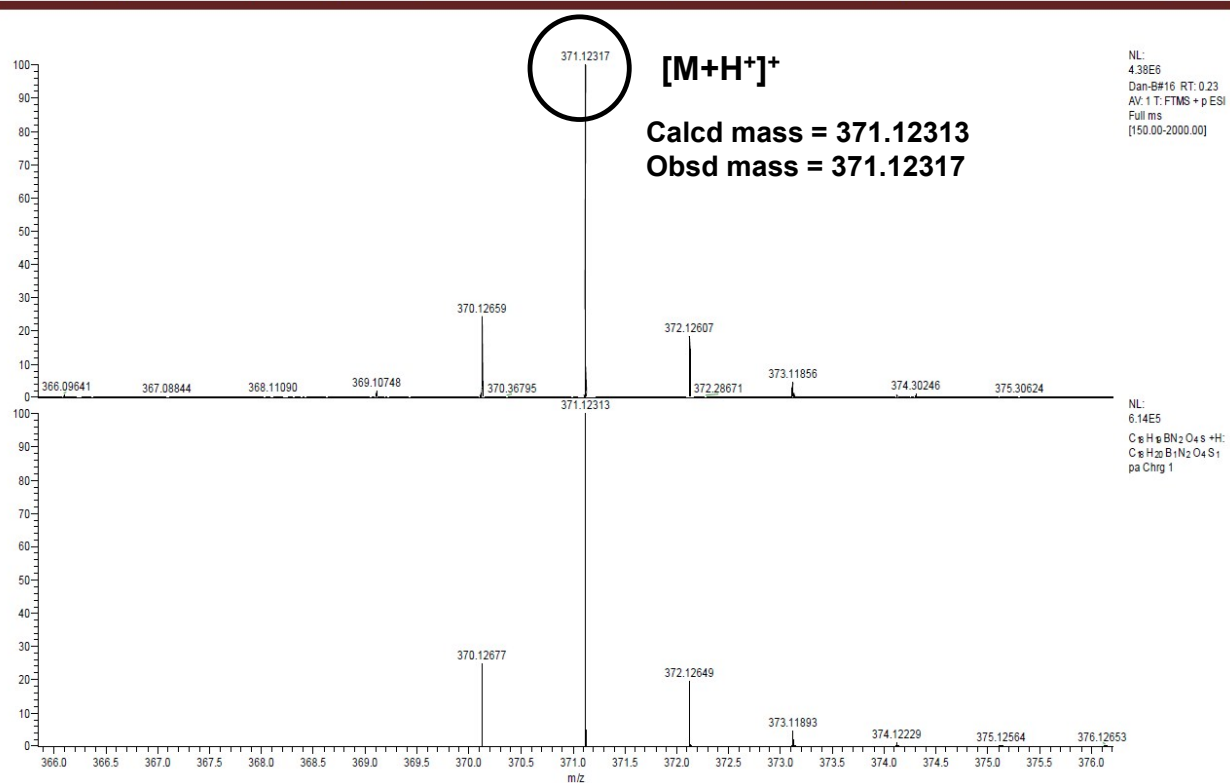


Figure S3. HR Mass Spectrum of **1**.

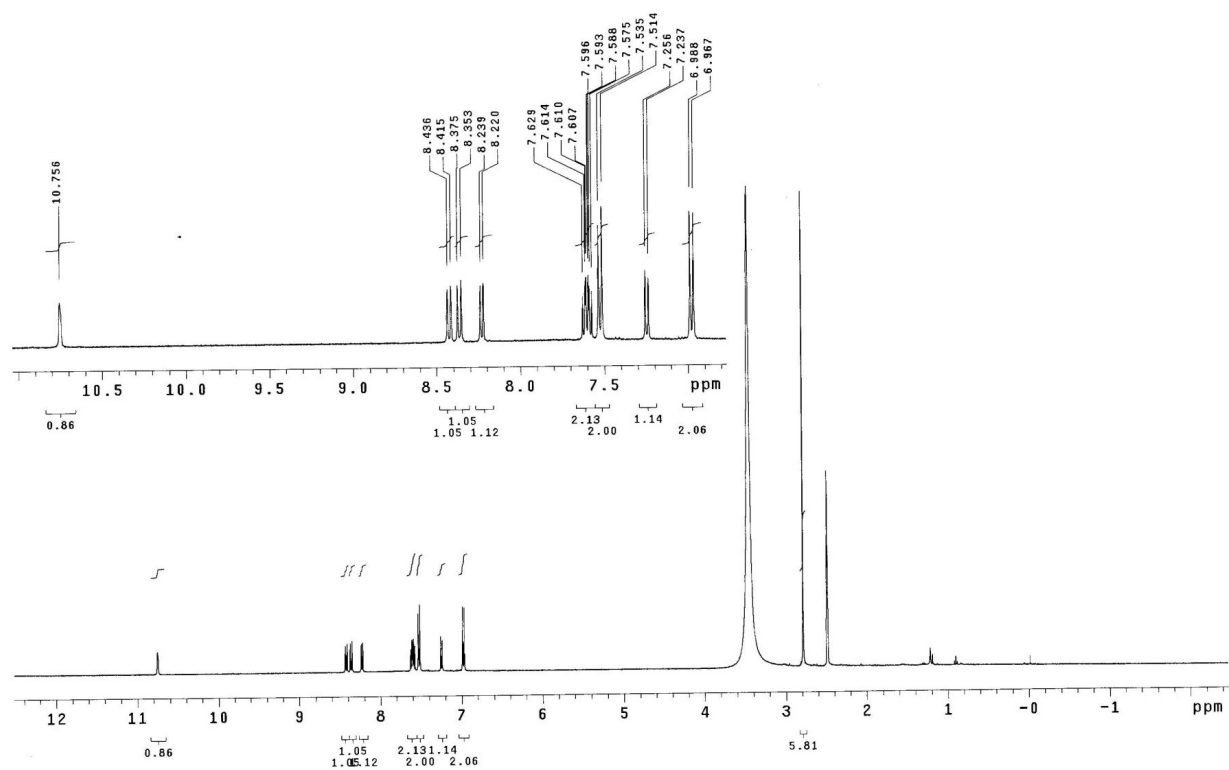


Figure S4. ¹H NMR of 1.

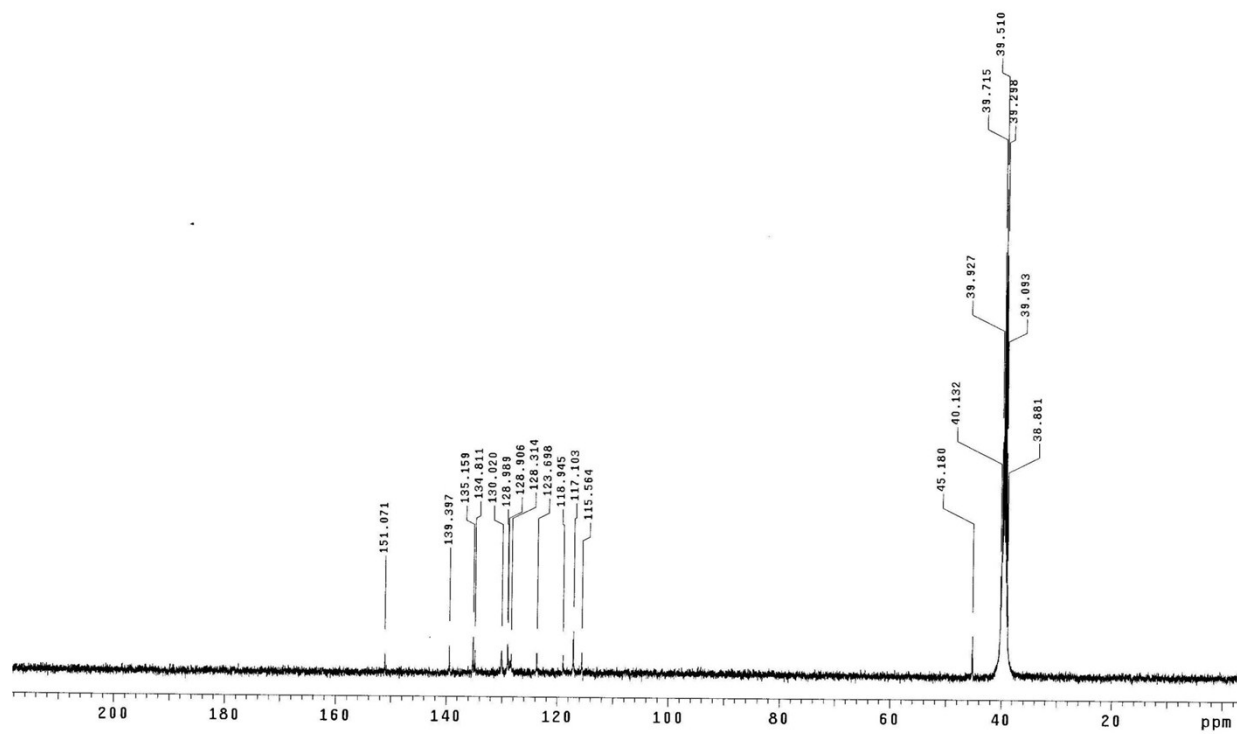


Figure S5. ¹³C NMR of 1.

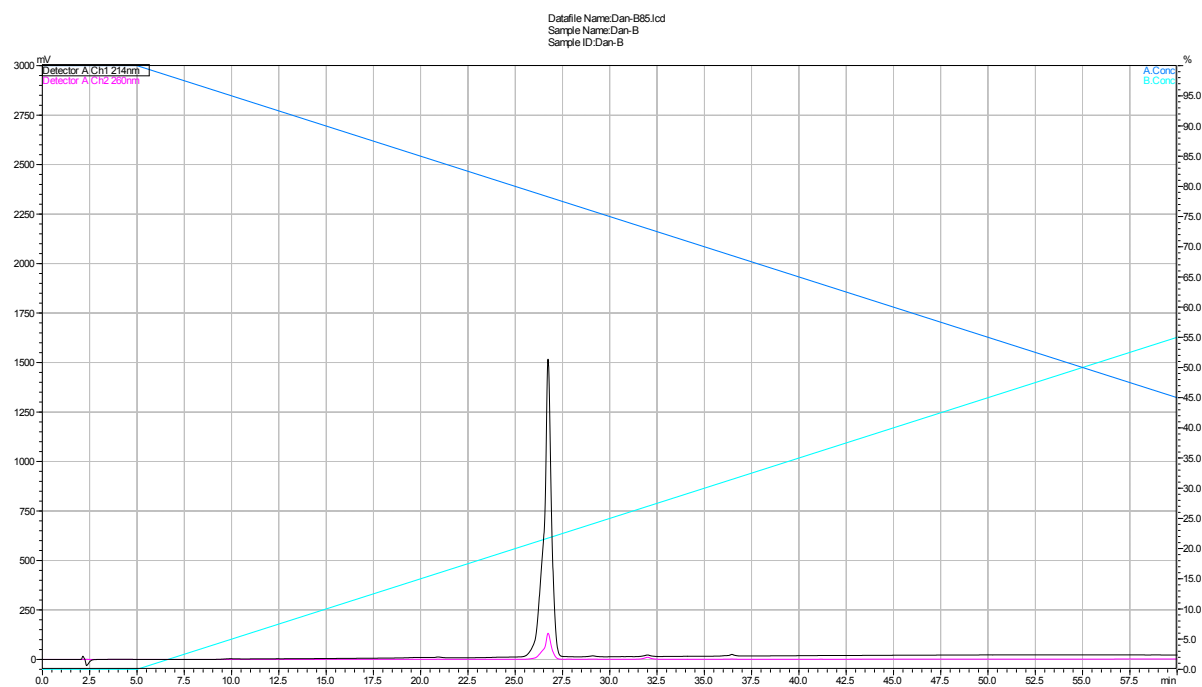


Figure S6. HPLC chromatogram of **2**. Black line and red line indicated the absorbance at 214 nm and 280 nm, respectively.

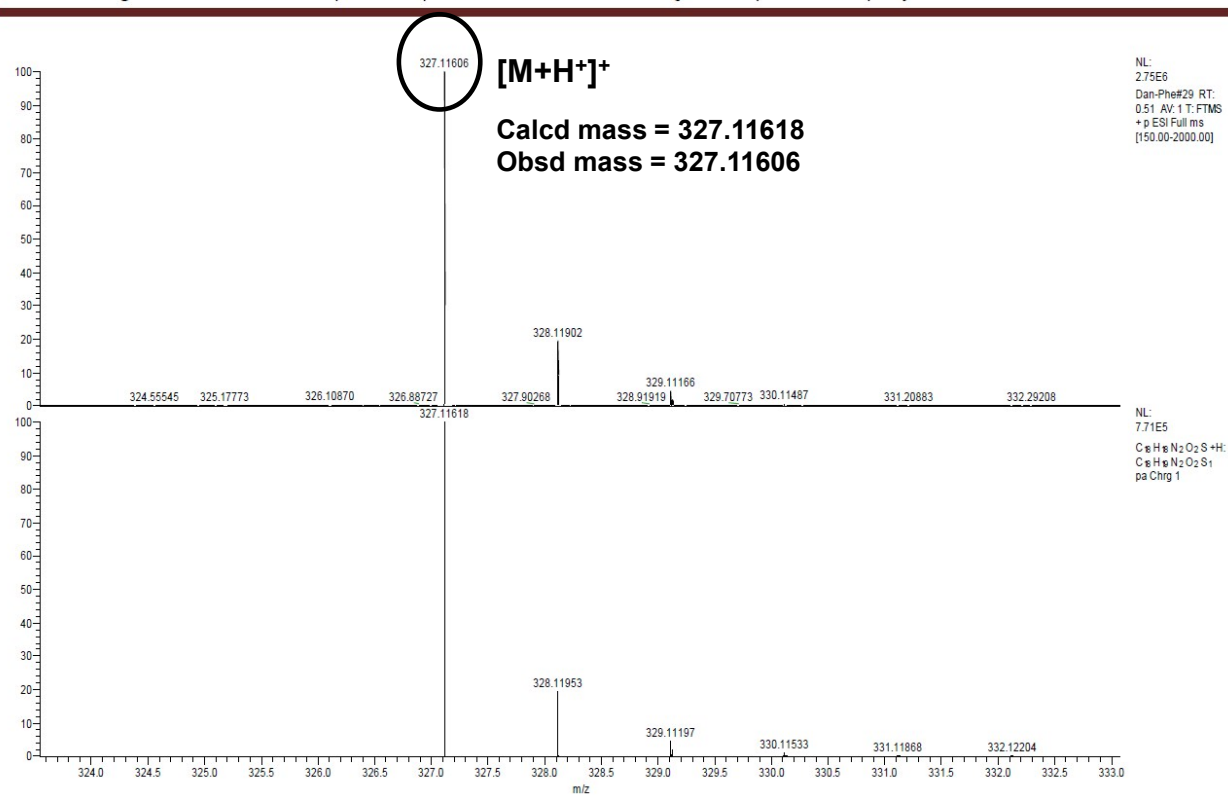


Figure S7. HR Mass Spectrum of **2**.

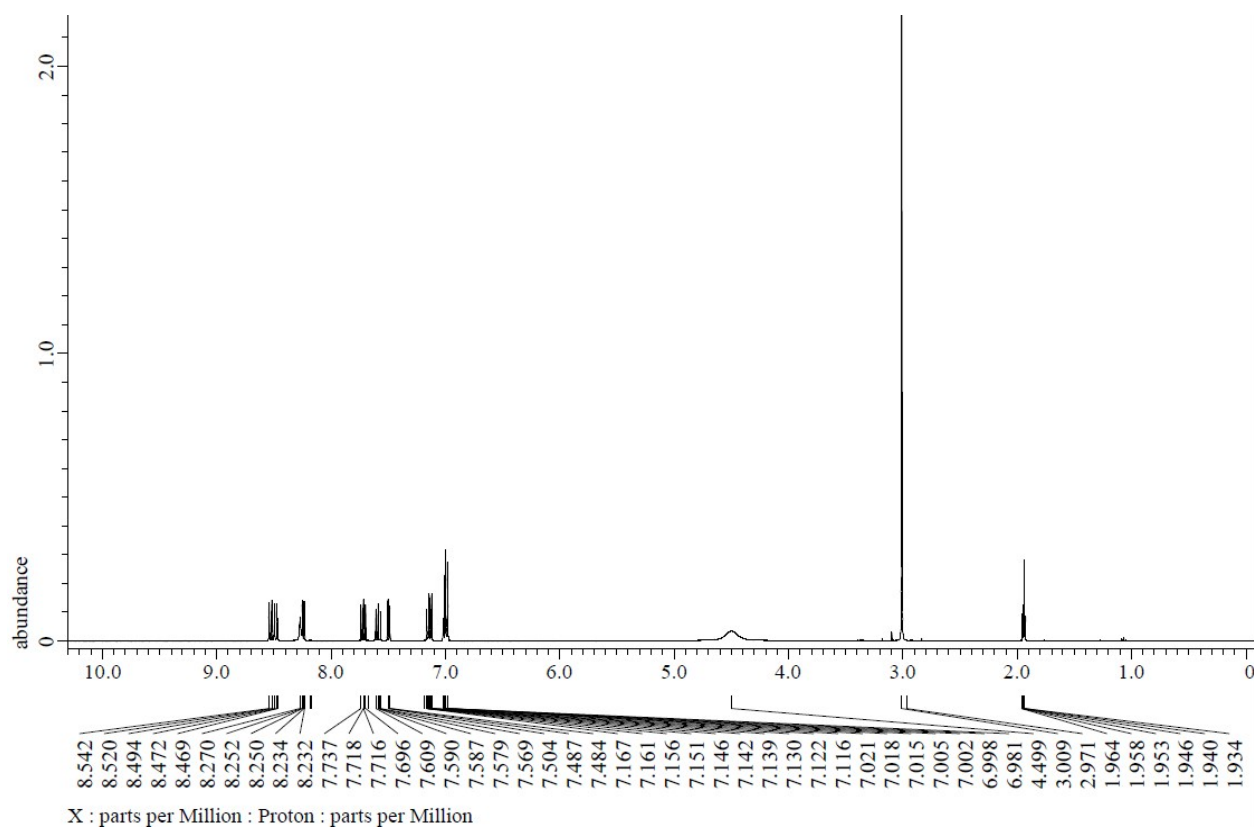


Figure S8. ^1H NMR of **2**.

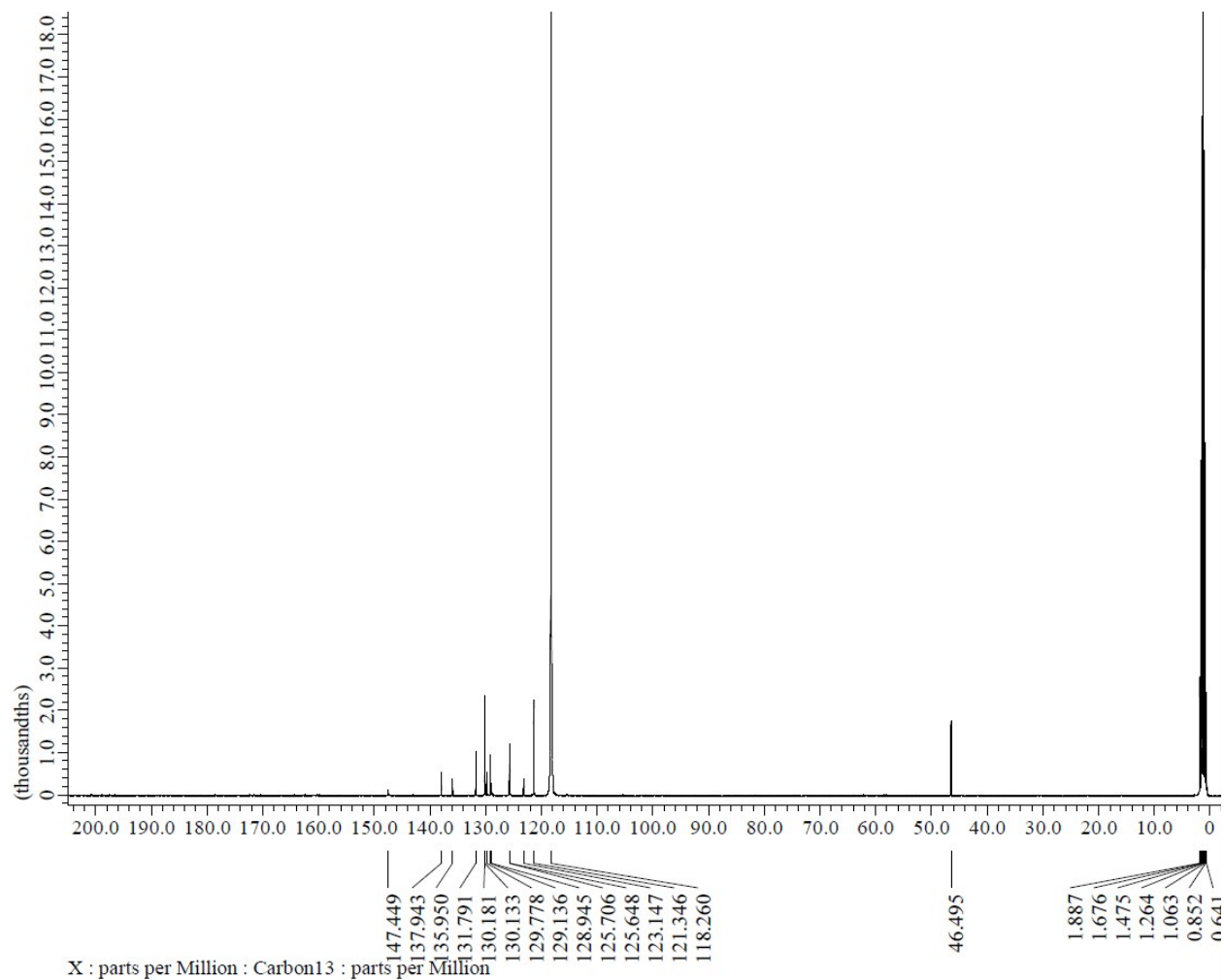


Figure S9. ^{13}C NMR of **2**.

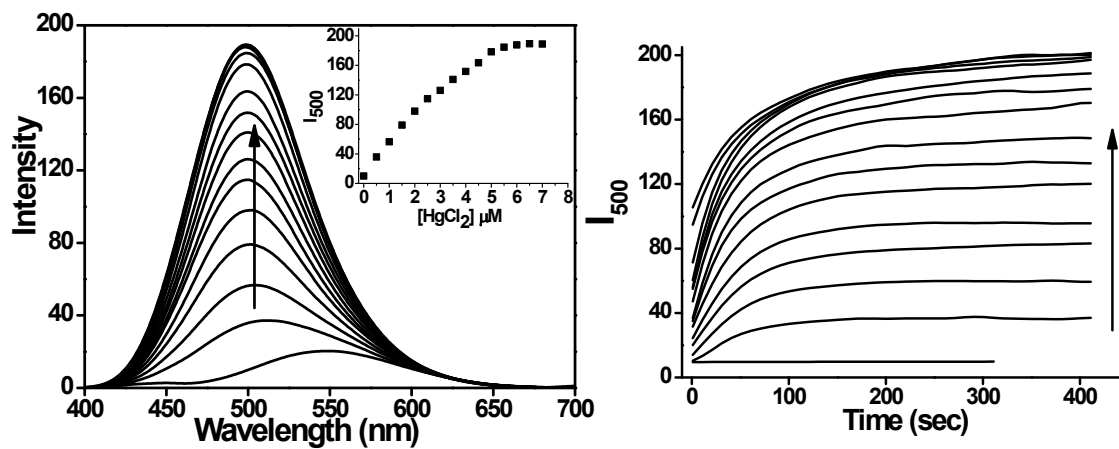


Figure S10. Fluorescent spectrum and time-dependent emission intensity at 500 nm of **1** (10 μM) with Hg^{2+} (0-0.7 equiv.) in (a) water- CH_3CN (99/1, v/v) and (b) aqueous buffered solution (10 mM HEPES, pH 7.4) containing 1% CH_3CN ($\lambda_{\text{ex}} = 380$ nm).

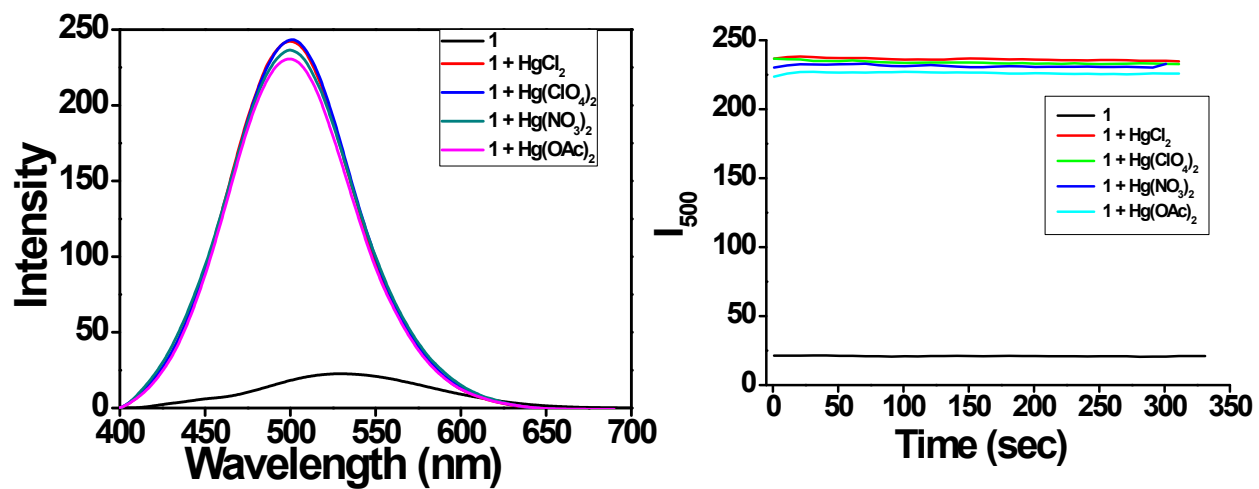


Figure S11. Fluorescent spectrum and time-dependent emission intensity at 500 nm of **1** (10 μM) with various mercury salts (1 equiv) in aqueous buffered solution (10 mM HEPES) at pH 7.4 containing 1% (v/v) CH₃CN (λ_{ex} = 380 nm).

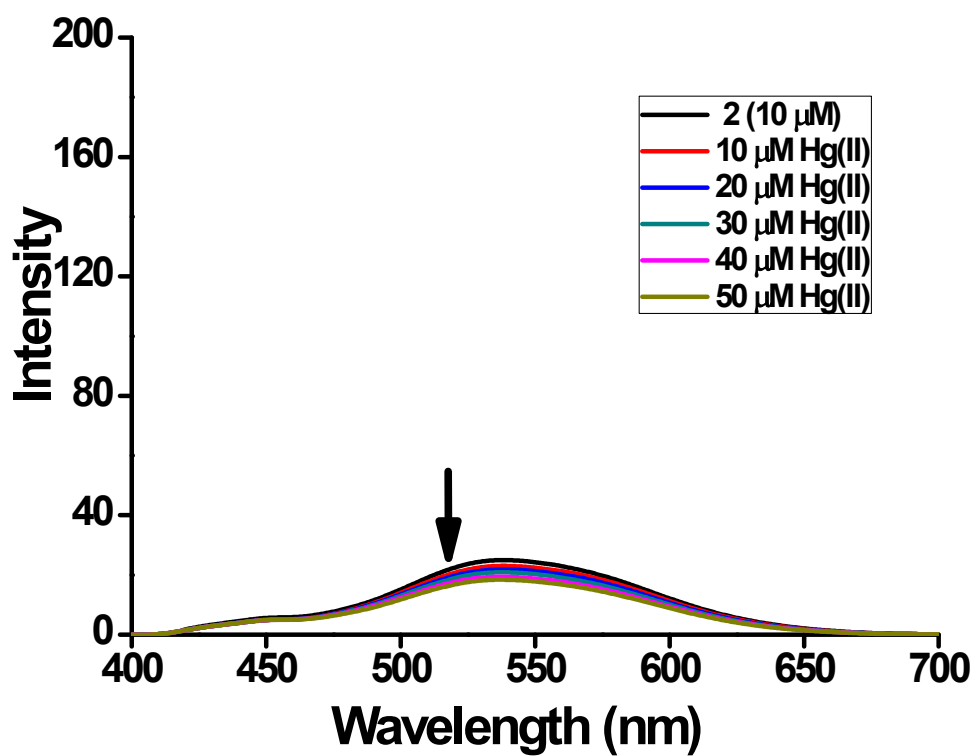


Figure S12. Fluorescent spectrum of **2** (10 μM) with HgCl_2 in aqueous buffered solution (10 mM HEPE) at pH 7.4 containing 1% (v/v) CH_3CN ($\lambda_{\text{ex}} = 380 \text{ nm}$).

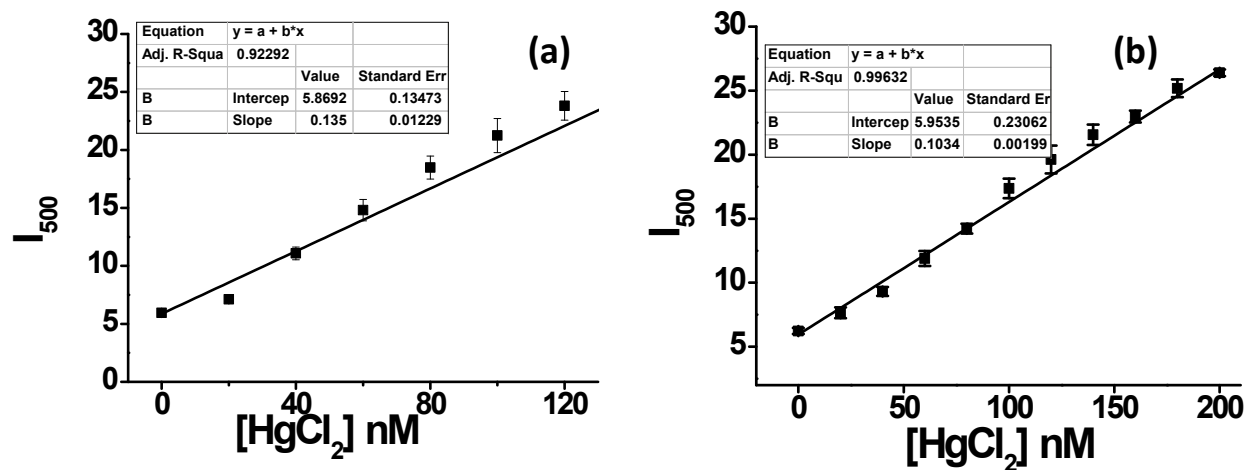


Figure S13. Linear emission intensity change of (a) **1** (2 μM) as a function of HgCl_2 in distilled water including 0.5% CH_3CN (b) **1** (500 nM) as a function of HgCl_2 in aqueous buffered solution (10 mM HEPE) at pH 7.4 including 0.5% CH_3CN .

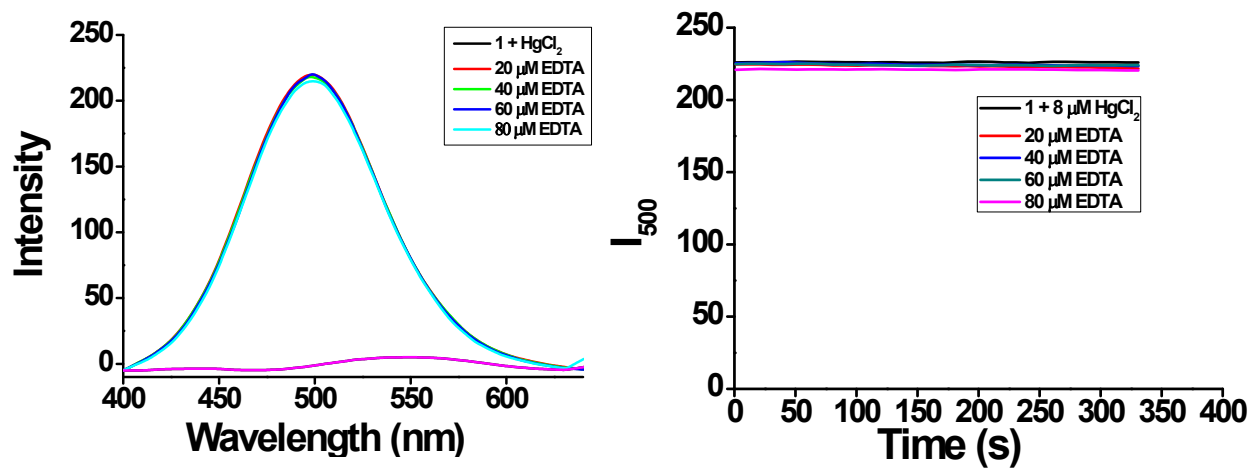


Figure S14. Fluorescent spectrum and time-dependent emission intensity at 500 nm of **1** (10 μM) with Hg^{2+} (0.8 equiv, 8 μM) and sequential addition of EDTA (20, 40, 60, and 80 μM) after 10 min incubation in aqueous buffered solution (10 mM HEPE) at pH 7.4 containing 1% CH_3CN .

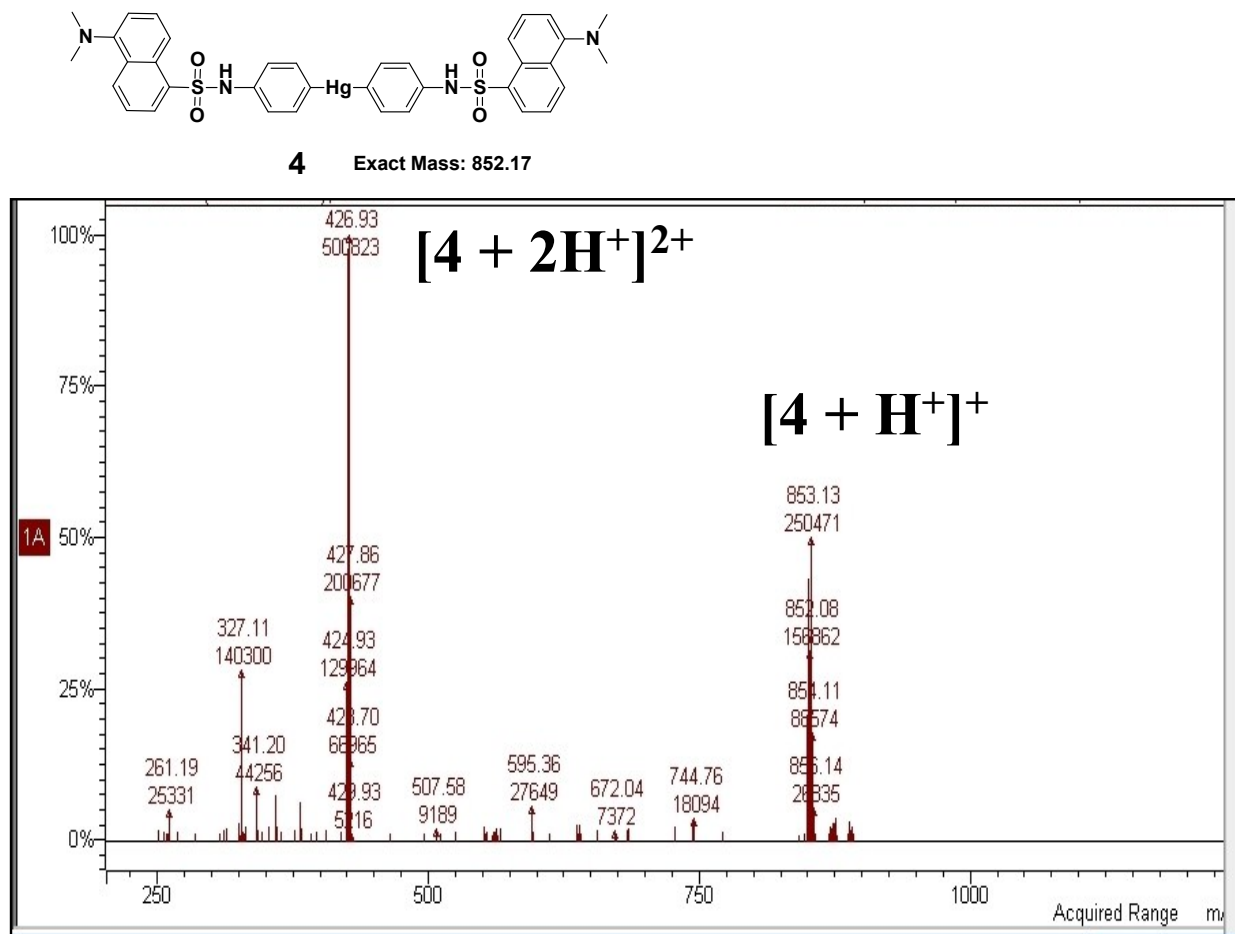


Figure S15. Mass spectrum of the peak at 52 min with positive ion mode.

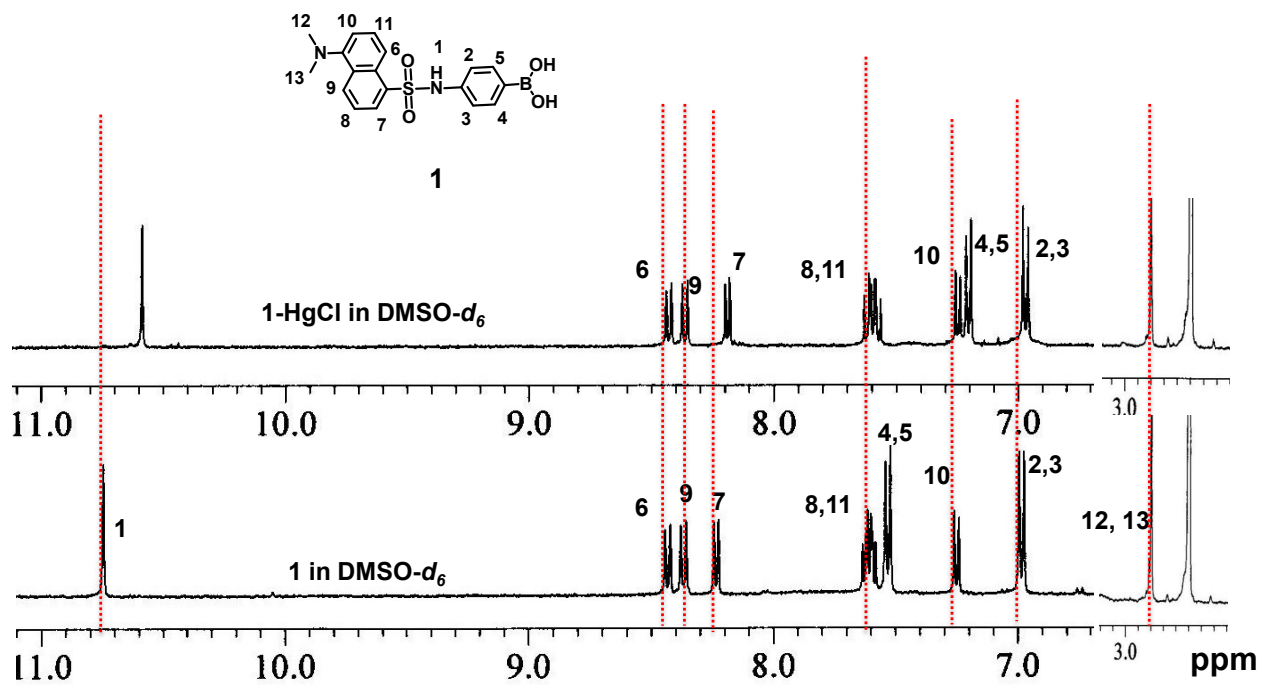


Figure S16. Partial ^1H NMR spectra (400 MHz) of **1** (3 mM) in the presence of HgCl_2 (1 equiv) in $\text{DMSO}-d_6$.

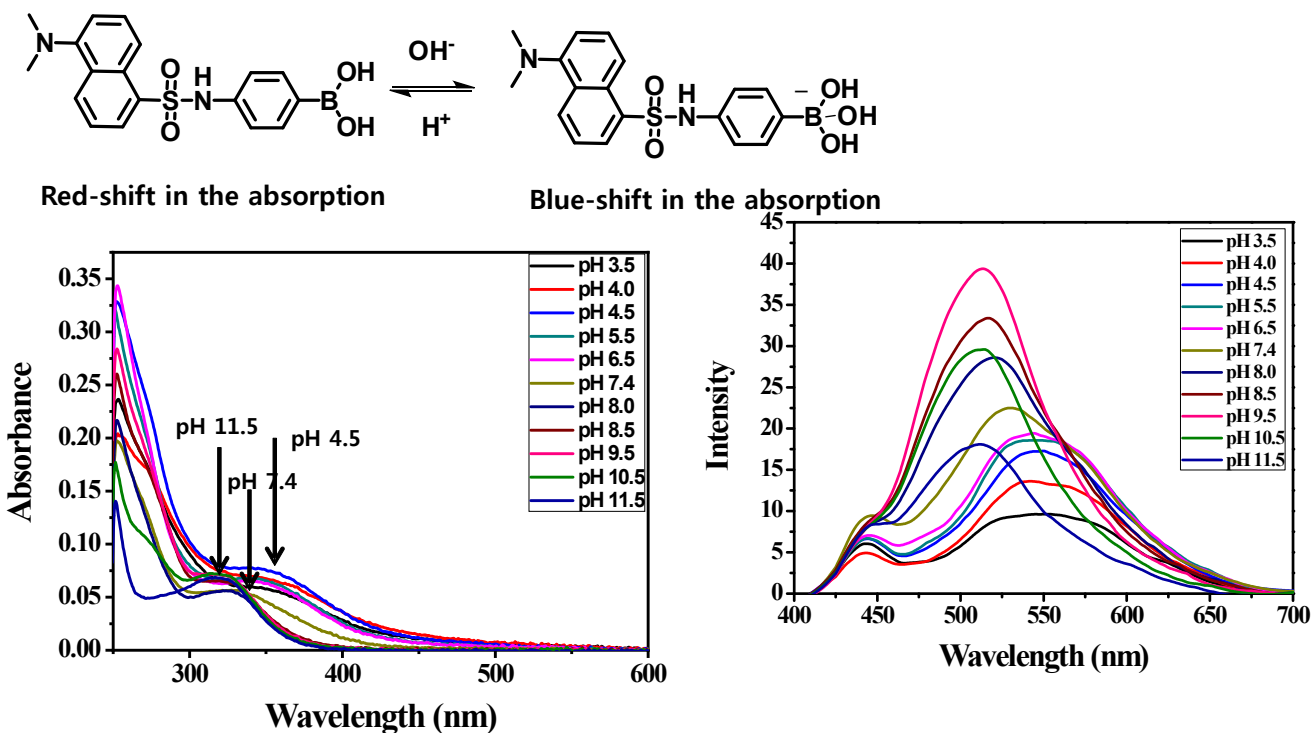


Figure S17. UV-visible spectrum and emission spectrum of **1** (10 μM) in aqueous buffered solution at various pHs (Acetate, pH 3.5–4.0; MES, pH 4.5–5.5; HEPES, pH 6.5–8.0; CHES, 8.5–11.5). The excitation wavelength was 380 nm.

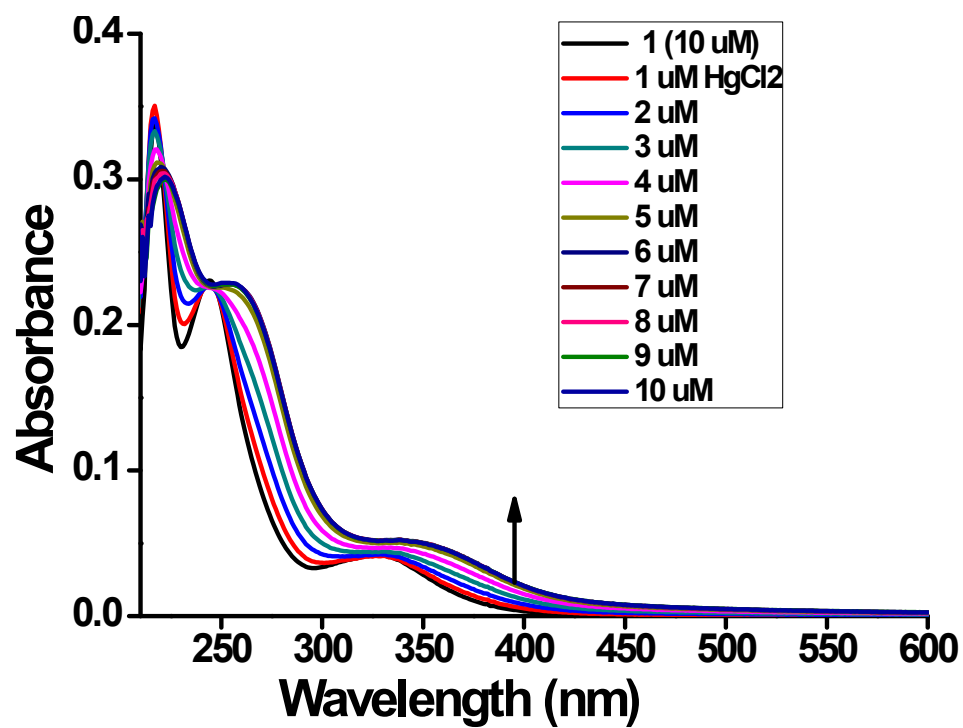


Figure S18. UV-visible spectrum of **1** (10 μM) with HgCl_2 in distilled water containing 1% CH_3CN .

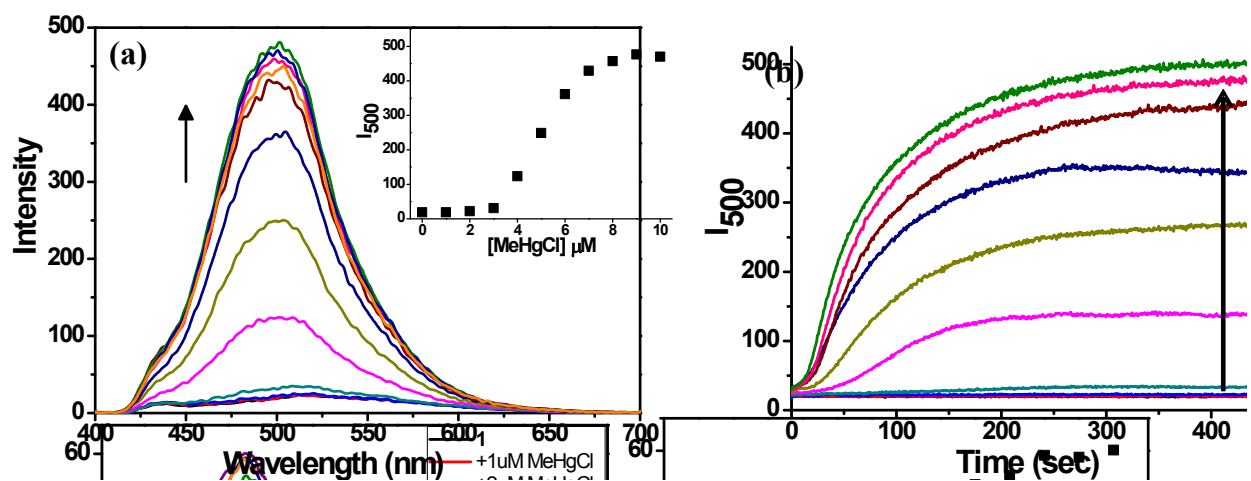


Figure S19. (a) Fluorescent spectrum and (b) time-dependent emission intensity of **1** (10 μM) with CH₃HgCl (0-1.0 equiv.) in aqueous buffered solution (10 mM HEPES, pH 7.4) containing 1% CH₃CN. The emission intensity was acquired 5 mins after addition of CH₃HgCl (λ_{ex} = 380 nm).

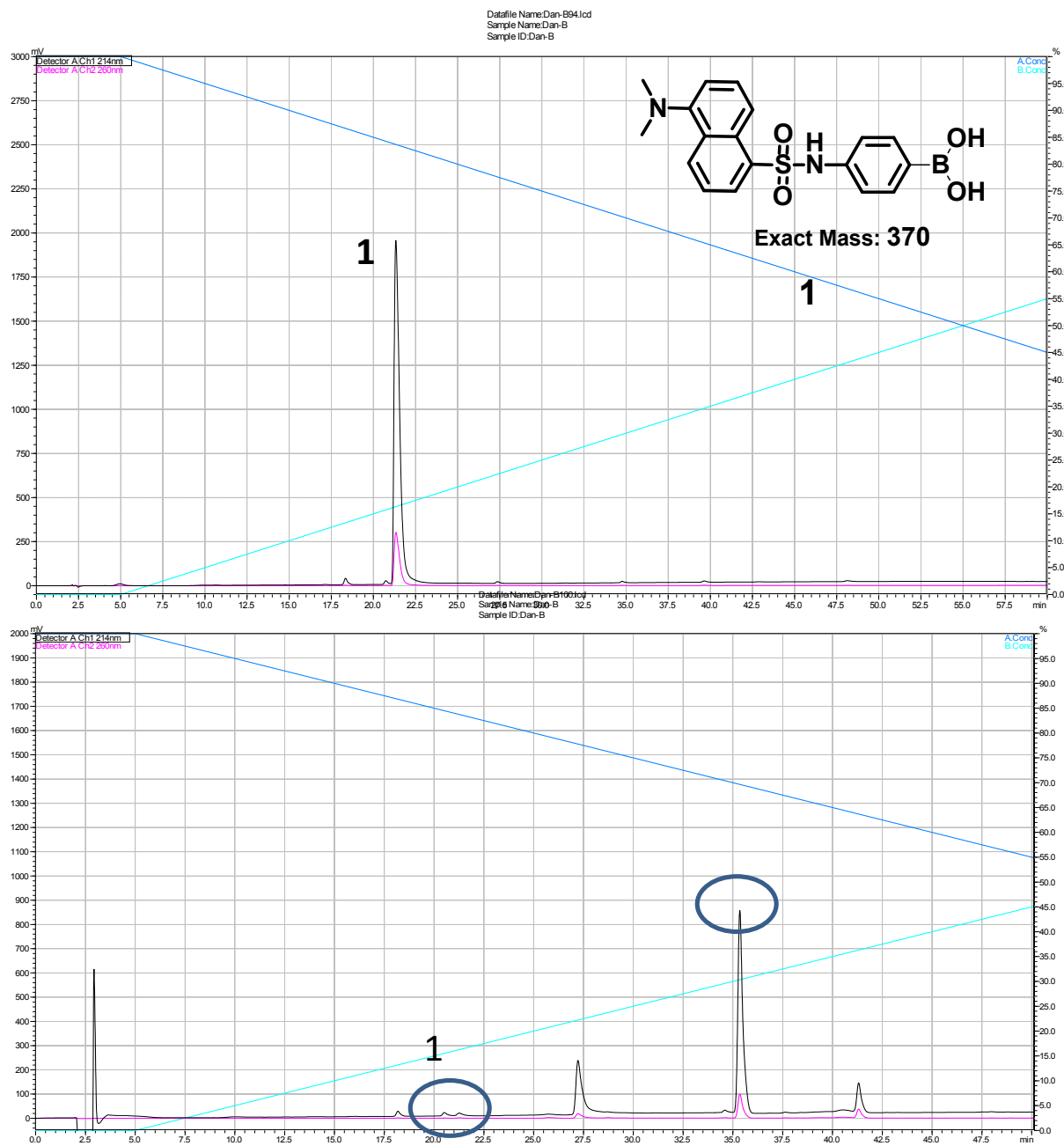


Figure S20. HPLC analysis using C₁₈ column of (a) **1** and (b) **1** with CH₃HgCl (1.0 equiv) incubated in distilled water containing 2% CH₃CN. Black line and red line indicated the absorbance at 214 nm and 280 nm, respectively.

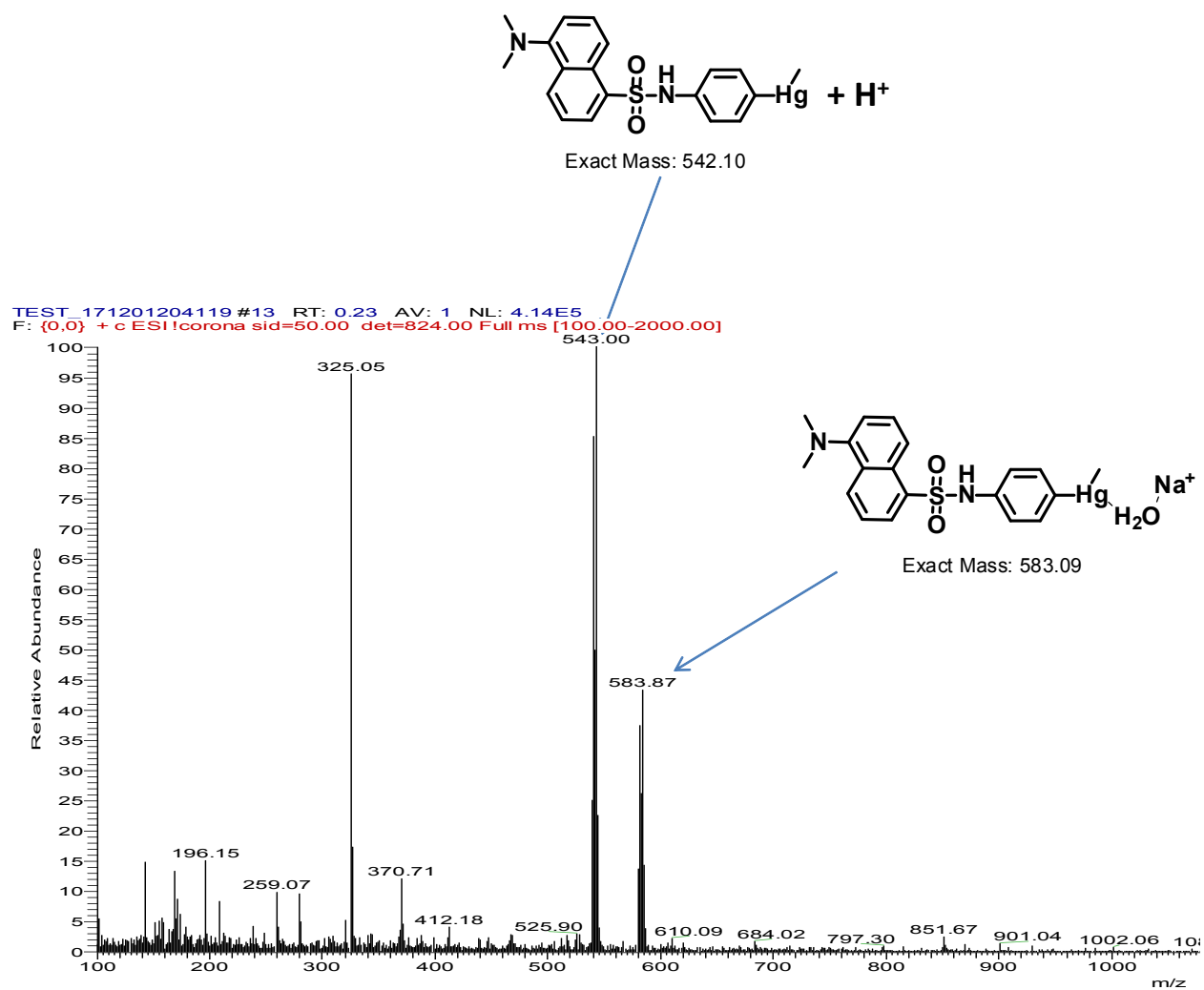


Figure S21. Mass spectrum of the peak at 35.5 min with positive ion mode and a possible product structure of the displacement reaction of **1** with CH_3HgCl .

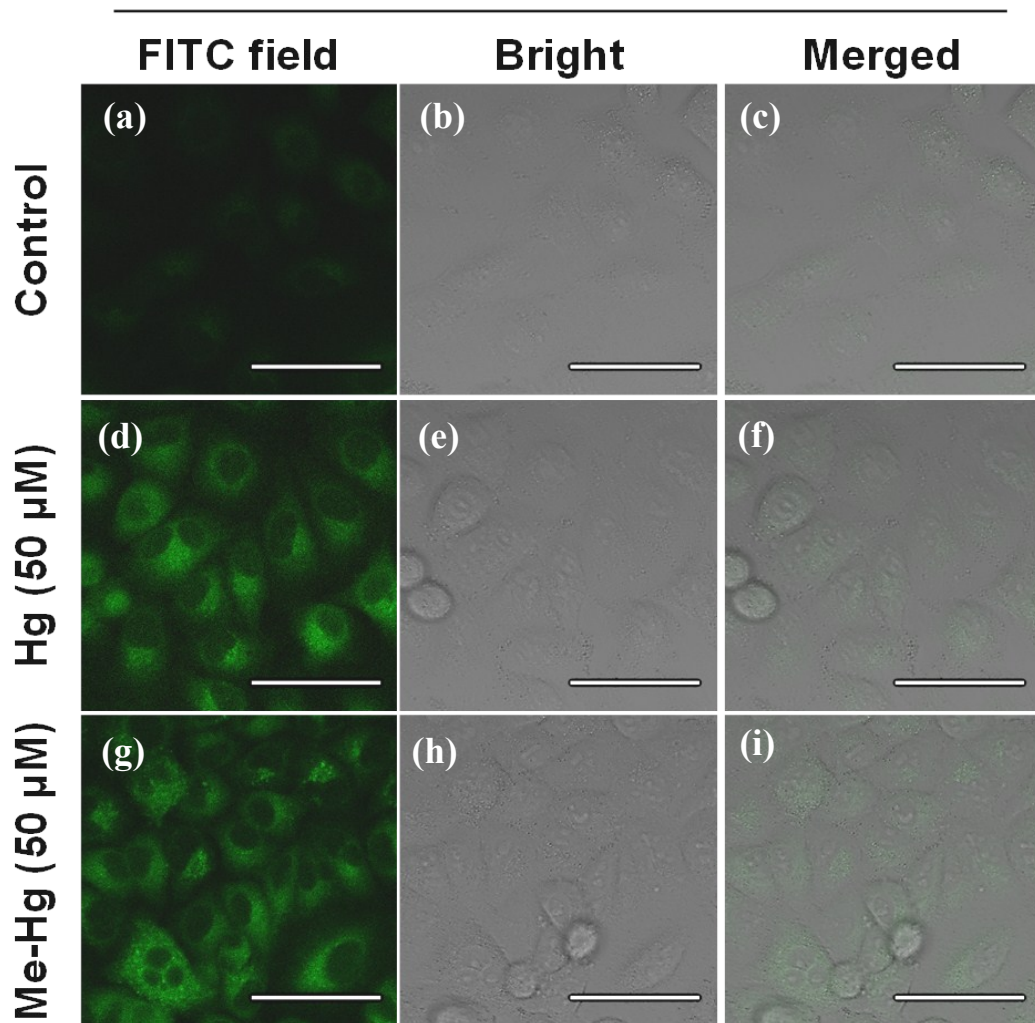


Figure S22. Confocal fluorescence images of A549 cells incubated with **1** (30 μ M) (top), and further incubated with HgCl_2 (50 μ M) (middle), and CH_3HgCl (50 μ M), bright-field images (a, d, g), confocal fluorescent images (b, e, h) and merged images (c, f, i). The emission intensities collected in optical windows between 490 and 550 nm [Scale bar = 20 μ m].

Table S1. Comparison of the detection properties of fluorescent probes for methylmercury

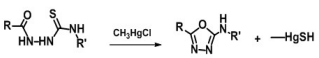
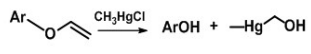
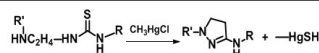
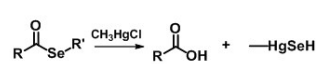
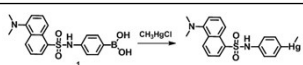
Reaction with methylmercury	Solvent	Emission wavelength (nm)	Saturation (equiv.)	Reaction Time (equiv. of CH_3Hg^+)	Ref.
	$\text{H}_2\text{O}/\text{DMSO}$ 99/1 (v/v)	560 nm	8	20 min (10 eq.)	1
	$\text{H}_2\text{O}/\text{DMSO}$ 95/5 (v/v)	520 nm	1	100 min (1 eq.)	2
	$\text{H}_2\text{O}/\text{EtOH}$ 1:4 (v/v)	660~800 nm	8	20 min (8 eq.)	3
	$\text{H}_2\text{O}/\text{ACN}$ 99/1 (v/v)	580 nm	10	10 min (10 eq.)	4
	$\text{H}_2\text{O}/\text{ACN}$ 99/1 (v/v)	500~550 nm	1	5 min (1 eq.)	This work

Table S2. The absorption and fluorescence maximum of 4 and 3 in various solvents at room temperature

Solvent (ϵ)	4		3	
	$\lambda_{\text{abs}}(\text{nm})$	$\lambda_{\text{em}}(\text{nm})$	$\lambda_{\text{abs}}(\text{nm})$	$\lambda_{\text{em}}(\text{nm})$
Toluene (2.38)	345	486.5	341.5	483.5
THF (7.52)	341	497.5	342	493.5
DCM (8.93)	345.5	510.5	348.5	510.5
MeOH (33.0)	340.5	518.5	340.5	518
ACN (36.6)	343	518	344	518
DMF (38.3)	345	518	343.5	517
DMSO (47.2)	346	517.5	346.5	520

References

1. Y. K. Yang, S. K. Ko, I. Shin, J. Tae, *Org. Biomol. Chem.*, 2009, **7**, 4590.
2. M. Santra, D. Ryu, A. Chatterjee, S. K. Ko, I. Shin, K. H. Ahn, *Chem. Commun.*, 2009, 2115.
3. Y. Liu, M. Chen, T. Cao, Y. Sun, C. Li, Q. Liu, T. Yang, L. Yao, W. Feng, F. Li, *J. Am. Chem. Soc.*, 2013, **135**, 9869.
4. X. Chen, K. H. Baek, Y. Kim, S. J. Kim, I. Shin, J. Yoon, *Tetrahedron*, 2010, **66**, 4016.